한국전산구조공학회
2004년도 가을 학술발표회 논문집

레벨 셋 기법을 이용한 에너지 흐름 문제의 형상 최적화

Shape Optimization of Energy Flow Problems Using Level Set Method

하 승 현* 박 찬 영* 조 선 호†
Ha, Seung-Hyun Park, Chan-Young Cho, Seonho

ABSTRACT

Using a level set method we develop a shape optimization method applied to energy flow problems in steady state. The boundaries are implicitly represented by the level set function obtainable from the "Hamilton-Jacobi type" equation with the "Up-wind scheme." The developed method defines a Lagrangian function for the constrained optimization. It minimizes a generalized compliance, satisfying the constraint of allowable volume through the variations of implicit boundary. During the optimization, the boundary velocity to integrate the Hamilton-Jacobi equation is obtained from the optimality condition for the Lagrangian function. Compared with the established topology optimization method, the developed one has no numerical instability such as checkerboard problems and easy representation of topological shape variations.

1. ENERGY FLOW PROBLEMS

Consider a structural body occupying an open domain Ω bounded by a closed surface Γ as shown in Figure 1. All the material properties are assumed homogeneous and isotropic in the domain Ω. Boundaries are composed of an energy boundary Γ^e and a flux boundary Γ^q such that

$$\Gamma^e \cup \Gamma^q = \Gamma \quad \text{and} \quad \Gamma^e \cap \Gamma^q = \phi . \tag{1}$$

The body is subjected to the rate of internal energy generation π and the following boundary conditions. A prescribed energy density e_0 on Γ^e and a prescribed energy flux q_0 on Γ^q in the inward normal direction are imposed. $\mathbb{m}$ is an outward unit vector normal to the boundary.

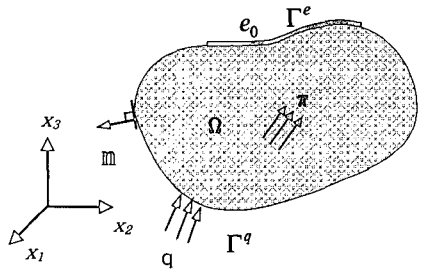

Figure 1 Structural body in space

For the energy field e, the governing equation for energy flow problems in steady state is written by

$$-\frac{c_g^2}{\eta\omega}\nabla^2 e + \eta\omega e = \pi , \tag{2}$$

where e, η, ω, and c_g are the time- and space-averaged energy density function, hysteresis damping factor, exciting frequency, and group speed, respectively. For plate structures, the group velocity is defined by

$$c_g = 2\times \sqrt[4]{\frac{\omega^2 D}{\rho h}} = 2\times \sqrt[4]{\frac{\omega^2 E h^2}{12\rho(1-\nu^2)}}, \tag{3}$$

* 학생회원, 서울대학교 조선해양공학과 석사과정
† 정회원, 서울대학교 조선해양공학과 교수

where ρ, ν, h, and D are the density, Poisson ratio, thickness, and flexural rigidity of plate, respectively. The boundary conditions are imposed as

$$e = e_0 \quad \text{on} \quad \Gamma^e \tag{4}$$

and

$$q = q_0 \quad \text{on} \quad \Gamma^q . \tag{5}$$

The space Z for trial solutions and $\overline{Z}$ for virtual fields are defined, respectively, as

$$Z = \{ e \in [H^1(\Omega)]^d : e = e_0 \quad \text{on} \quad \Gamma^e \} \tag{6}$$

and

$$\overline{Z} = \{ \bar{e} \in [H^1(\Omega)]^d : \bar{e} = 0 \quad \text{on} \quad \Gamma^e \} . \tag{7}$$

where d represents the dimension of problem and $H^1(\Omega)$ is the Hilbert space of order one. Using the virtual field $\bar{e}$ that satisfies a homogeneous Dirichlet boundary condition, the weak form of the Equation (2) is written, using the divergence theorem, as

$$\int_\Omega \left(\frac{c_g^2}{\eta\omega} \nabla e \cdot \nabla \bar{e} + \eta\omega e \bar{e} \right) d\Omega = \int_\Omega \pi \bar{e} d\Omega - \int_{\Gamma_q} q \bar{e} d\Gamma \quad \text{for all} \quad \bar{e} \in \overline{Z} , \tag{8}$$

where a time- and space-averaged energy intensity $\mathbf{I}$ and an energy flux q are defined by

$$\mathbf{I} = -\frac{c_g^2}{\eta\omega} \nabla e \tag{9}$$

$$q = \mathbf{n} \cdot \mathbf{I} , \tag{10}$$

Defining a bilinear form

$$a(e, \bar{e}) \equiv \int_\Omega \left(\frac{c_g^2}{\eta\omega} \nabla e \cdot \nabla \bar{e} + \eta\omega e \bar{e} \right) d\Omega \tag{11}$$

and a linear form

$$\ell(\bar{e}) \equiv \int_\Omega \pi \bar{e} d\Omega - \int_{\Gamma_q} q \bar{e} d\Gamma , \tag{12}$$

the Equation (8) can be rewritten as

$$\text{Find} \quad e \in Z \quad \text{such that} \quad a(e, \bar{e}) = \ell(\bar{e}) \quad \text{for all} \quad \bar{e} \in \overline{Z} . \tag{13}$$

2. LEVEL SET FORMULATION

Let $\Omega \subset R^d$ be a bounded open domain with a smooth boundary Γ, at a generic configuration, as

$$\Omega = \Omega_N \cup \Omega_D , \tag{14}$$

where Ω_N and Ω_D are a non-designable and a designable domains, respectively. Imagine the boundary of domain Γ moves in the direction normal to its boundary with a known speed V_n. To derive the equation of moving boundary as time evolves, we embed this propagating boundary as the zero level set ϕ of a $(d+1)$-dimensional function $\Phi(\phi, k)$. Let Γ_I and Ω_I be an initial reference boundary and domain, respectively. At time $\tau = 0$, assume the existence of a zero level set function $\phi(\mathbf{x}, 0)$ that is Lipschitz continuous and defined on Ω_I, satisfying

$$\phi(\mathbf{x}, \tau = 0) \begin{cases} +\zeta(\mathbf{x}, \Gamma) & \mathbf{x} \in \Omega \\ = 0 & \mathbf{x} \in \Gamma \\ -\zeta(\mathbf{x}, \Gamma) & \mathbf{x} \in \Omega_I \setminus \overline{\Omega} \end{cases} \tag{15}$$

where $\zeta(\mathbf{x}, \Gamma)$ is a distance from a point $\mathbf{x}$ to the boundary Γ, for all $\mathbf{x} \in R^d$. Also let Γ_τ and Ω_τ be a moving boundary and a corresponding domain at time τ, respectively.

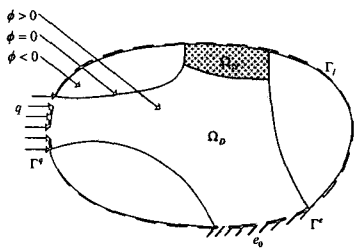

Figure 2 Design domains and level set function

An outward unit vector $\mathbb{m}$ normal to the boundary Γ is obtained by

$$\mathbb{m} = -\frac{\nabla\phi}{|\nabla\phi|}. \tag{16}$$

and a curvature κ is defined by the divergence of $\mathbb{m}$, as

$$\kappa = div\,\mathbb{m} = -\nabla\cdot\left(\frac{\nabla\phi}{|\nabla\phi|}\right). \tag{17}$$

We employ the level set method for the implicit representation of boundaries. At arbitrary time, the level set model describes a surface in implicit form at zero level as the iso-surface of a scalar function $\phi : R^2 \rightarrow R$ embedded in three dimensional space, as

$$S = \{\, \mathbb{x} : \phi(\mathbb{x},0) = k \,\}, \tag{18}$$

where k and $\mathbb{x}$ are an arbitrary iso-value and a point on the iso-surface ϕ, respectively. Taking the material derivative of level set function with respect to the parameter τ leads to the "Hamilton-Jacobi type equation" as

$$\frac{D\phi}{D\tau} \equiv \left.\frac{\partial\phi(\mathbb{x}_\tau,\tau)}{\partial\tau}\right|_{\tau=0} + \nabla\phi(\mathbb{x}_\tau,\tau)\big|_{\tau=0}\cdot\left.\frac{d\mathbb{x}_\tau}{d\tau}\right|_{\tau=0} = \frac{\partial\phi(\mathbb{x},0)}{\partial\tau} + \nabla\phi(\mathbb{x},0)\cdot\frac{d\mathbb{x}}{d\tau} = 0. \tag{19}$$

Note that the transportation of level set function ϕ is defined in the Lagrangian frame whereas the variation of ϕ in the Eulerian frame. The mapping between two level set models, i.e. $T(\mathbb{x},\tau) : \mathbb{x} \rightarrow \mathbb{x}_\tau(\mathbb{x})$, $\mathbb{x} \in \Omega$, yields the design velocity field for the shape optimization as

$$\mathbb{x}_\tau \equiv T(\mathbb{x},\tau) = \mathbb{x} + \tau\mathbb{V}(\mathbb{x},0) + \ldots, \tag{20}$$

$$\frac{d\mathbb{x}}{d\tau} \equiv \lim_{\tau\to 0}\frac{\mathbb{x}_\tau - \mathbb{x}}{\tau} = \mathbb{V}(\mathbb{x},0) = \mathbb{V}(\mathbb{x}) \quad . \tag{21}$$

Thus, the Equation (19) is rewritten by

$$\frac{\partial\phi(\mathbb{x},0)}{\partial\tau} = -\nabla\phi(\mathbb{x},0)\cdot\mathbb{V}(\mathbb{x})\cdot \tag{22}$$

Let V_n be a speed function normal to the boundary. Using the Equation (16), we have the following.

$$V_n = \mathbb{V}\cdot\mathbb{n} = -\mathbb{V}(x)\cdot\frac{\nabla\phi}{|\nabla\phi|}\cdot \tag{23}$$

Substituting the Equation (23) into the Equation (22) and applying appropriate boundary conditions yield the following equations as

$$\frac{\partial\phi}{\partial\tau} = V_n|\nabla\phi|, \quad \left.\frac{\partial\phi}{\partial n}\right|_{\Gamma_t} = 0\cdot \tag{24}$$

Given a normal velocity field $V_n(\mathbb{x})$, we can update the level set function $\phi(\mathbb{x})$ at each time step by solving the first order partial differential equation with initial values as shown in Equation (24). For computational stability, the "Up-wind scheme" (Sethian; 1999) is employed.

$$\phi_{ij}^{n+1} = \phi_{ij}^{n} + \Delta t\left[\max\{-(V_n)_{ij},0\}\nabla^{+} + \min\{-(V_n)_{ij},0\}\nabla^{-}\right], \tag{25}$$

where

$$\nabla^+ = \left\{\max(D_{ij}^{-x},0)^2 + \min(D_{ij}^{+x},0)^2 + \max(D_{ij}^{-y},0)^2 + \min(D_{ij}^{+y},0)^2\right\}^{\frac{1}{2}}, \tag{26}$$

$$\nabla^- = \left\{\max(D_{ij}^{+x},0)^2 + \min(D_{ij}^{-x},0)^2 + \max(D_{ij}^{+y},0)^2 + \min(D_{ij}^{-y},0)^2\right\}^{\frac{1}{2}}. \tag{27}$$

$D_{ij}^{\pm x}$, $D_{ij}^{\pm y}$, and Δt are the forward and backward difference operators on ϕ_{ij}^n and a time step, respectively. Embedding the obtained level set function ϕ into the Equation (13), the variational equation can be written as

$$\text{Find } e \in Z \text{ such that } a_\phi(e,\bar{e}) = \ell_\phi(\bar{e}) \text{ for all } \bar{e} \in \bar{Z}. \tag{28}$$

The bilinear and linear forms are expressed, respectively, as

$$a_\phi(e,\bar{e}) \equiv \int_{\Omega_I} \hat{H}(\phi)\left(\frac{c_g^2}{\eta\omega}\nabla e\cdot\nabla\bar{e} + \eta\omega e\bar{e}\right)d\Omega \tag{29}$$

$$\ell_\phi(\bar{e}) \equiv \int_{\Omega_I} \hat{H}(\phi)\pi\bar{e}\,d\Omega - \int_{\Omega_I} \delta(\phi)|\nabla\phi|q\bar{e}\,d\Omega. \tag{30}$$

3. SHAPE OPTIMIZATION

The objective of shape optimization is to find an optimal layout that minimizes the generalized compliance $\Pi_\phi(e)$ of the system under the prescribed loadings. The optimization problem is stated as

$$\text{Minimize } \Pi_\phi(e) \equiv \int_{\Omega_I} \hat{H}(\phi)\pi e\,d\Omega - \int_{\Omega_I} \delta(\phi)|\nabla\phi|qe\,d\Omega, \tag{31}$$

$$\text{Subject to } \int_{\Omega_I} \hat{H}(\phi)d\Omega \le M_{\max}, \tag{32}$$

where $M_{\max}$ is an allowable volume. The function ϕ, playing a role of the design variable and representing the current implicit boundary, is varying as

$$\phi_\tau = \phi + \tau\varphi,\ \varphi \in \Psi, \tag{33}$$

where φ indicates the direction of boundary variations and belongs to the function space Ψ.

$$\Psi = \{\,\varphi \in C^1(\Omega_I):\ \varphi = 0 \text{ on } \Gamma_I^e\,\}. \tag{34}$$

3.1 Adjoint design sensitivity analysis

Take Fréchet derivative of the Equation (28) with respect to τ in the direction of φ as

$$a_\phi(e',\bar{e}) = \ell'_\phi(\bar{e}) - a'_\phi(e,\bar{e}), \text{ for all } \bar{e} \in \bar{Z}, \tag{35}$$

where

$$a'_\phi(e,\bar{e}) \equiv \int_{\Omega_I} \delta(\phi)\left(\frac{c_g^2}{\eta\omega}\nabla e\cdot\nabla\bar{e} + \eta\omega e\bar{e}\right)\varphi d\Omega \tag{36}$$

and

$$\ell'_\phi(\bar{e}) \equiv \int_{\Omega_I} \delta(\phi)\left[\pi\bar{e} - \nabla\{q\bar{e}\}\cdot\mathrm{n} - \kappa\{q\bar{e}\}\right]\varphi d\Omega - \int_{\Gamma_I} \delta(\phi)q\bar{e}\,\varphi d\Gamma. \tag{37}$$

Consider a generalized compliance functional shown in Equation (31). Then, we come up with the sensitivity of the generalized compliance, taking advantage of Equation (37) as

$$\frac{d\Pi_\phi(e)}{d\tau} = \int_{\Omega_I} \hat{H}(\phi)\pi e'd\Omega - \int_{\Omega_I} \delta(\phi)|\nabla\phi|qe'd\Omega + \int_{\Omega_I} \delta(\phi)\left[\pi e - \nabla\{qe\}\cdot\mathrm{n} - \kappa\{qe\}\right]\varphi d\Omega - \int_{\Gamma_I} \delta(\phi)qe\varphi d\Gamma. \tag{38}$$

Using an adjoint equation, Equation (38) can be rewritten as

$$\frac{d\Pi_\phi(e)}{d\tau} = \int_{\Omega_I} \delta(\phi)\left[\pi(e+\lambda) - \nabla\{q(e+\lambda)\}\cdot\mathrm{n} - \kappa q(e+\lambda) - \left(\frac{c_g^2}{\eta\omega}\nabla e\cdot\nabla\lambda + \eta\omega e\lambda\right)\right]\varphi d\Omega + \int_{\Gamma_I} \delta(\phi)q(e+\lambda)\varphi d\Gamma$$

$$= \int_{\Omega_I} \delta(\phi)\Xi_\phi(e,\lambda)\varphi d\Omega + \int_{\Gamma_I} \delta(\phi)q(e+\lambda)\varphi d\Gamma. \tag{39}$$

Since the followings hold,

$$\delta(\phi(x)) = 0 \quad \text{for some} \quad x \notin \Gamma_I \tag{40}$$

and

$$\varphi \equiv \frac{\partial \phi}{\partial \tau} = \frac{\partial \phi}{\partial n}\frac{\partial n}{\partial \tau} = 0 \quad \text{for the other} \quad x \in \Gamma_I\,, \tag{41}$$

the Equation (39) can be rewritten as

$$\frac{d\Pi_\phi(e)}{d\tau} = \int_{\Omega_I} \delta(\phi)\Xi_\phi(e,\lambda)\varphi d\Omega. \tag{42}$$

3.2 Optimality conditions

The velocity field $V_n(x)$ defines the propagation speed of all level sets of the embedding function $\phi(\mathbb{x})$ along the outward normal direction. The velocity should be determined such that it reduces the generalized compliance of the system while satisfying the requirement of allowable material volume. Define a Lagrangian function Λ for the constrained optimization problems as

$$\begin{aligned}\Lambda(\phi,\mu,s) &= \Pi_\phi(e) + \mu\left\{m(\phi) + s^2 - M_{\max}\right\} \\ &= \int_{\Omega_I} \hat{H}(\phi)\pi e d\Omega - \int_{\Omega_I} \delta(\phi)|\nabla\phi| q e d\Omega + \mu\left\{\int_{\Omega_I} \hat{H}(\phi)d\Omega + s^2 - M_{\max}\right\},\end{aligned} \tag{43}$$

where $M_{\max}$, s, and μ are the allowable material volume, a slack variable to convert the inequality constraint to the equality one, and a Lagrange multiplier, respectively. Applying the Kuhn-Tucker optimality conditions leads to

$$\frac{d\Lambda(\phi,\mu,s)}{d\tau} = \int_{\Omega_I} \delta(\phi)\left\{\Xi_\phi(e,\lambda) + \xi\right\}\varphi d\Omega = 0\,, \tag{44}$$

where

$$\xi = \begin{cases} 0 & \text{if} \quad \int_{\Omega_I} \hat{H}(\phi)d\Omega < M_{\max} \\ \mu & \text{if} \quad \int_{\Omega_I} \hat{H}(\phi)d\Omega \geq M_{\max} \end{cases}, \quad \mu \geq 0 \tag{45}$$

3.3 Computation of velocity field

Now that the distance function $\phi(\mathbb{x})$ is normal to the boundary and the only normal velocity has influence on the result of shape optimization, the domain variation can be expressed, using the normal velocity $V_n(x)$.

$$\Omega_\tau = (\mathbb{I}d + \tau V_n)(\Omega_I)\,. \tag{46}$$

Using Taylor series expansion in the normal direction of velocity field, the perturbed Lagrangian function can be expressed as

$$\Lambda(\Omega_\tau) = \Lambda\left\{(\mathbb{I}d + \tau V_n)(\Omega_I)\right\} = \Lambda(\Omega_I) + \Lambda'(\Omega_I)(\tau V_n) + \cdots, \tag{47}$$

where the sensitivity of the Lagrangian function is expressed as

$$\Lambda'(\Omega_I) = \int_{\Omega_I} \delta(\phi)\left\{\Xi_\phi(e,\lambda) + \xi\right\}\varphi d\Omega\,. \tag{48}$$

If we take the boundary variation in the descent direction of the sensitivity as

$$V_n = -\left\{\Xi_\phi(e,\lambda) + \xi\right\}\varphi\,, \tag{49}$$

then the Equation (66) can be written as

$$\Lambda(\Omega_\tau) = \Lambda(\Omega_I) - \tau\int_{\Omega_I} \delta(\phi)\left\{\Xi(e,\lambda) + \xi\right\}^2\varphi^2 d\Omega + O(\tau^2) + \cdots, \tag{50}$$

Thus, the decrease of generalized compliance functional is guaranteed while satisfying the requirement of allowable material volume.

4. NUMERICAL EXAMPLES

In Figure 3, the design domain, boundary, and loading conditions for the two numerical models are illustrated. A thick line indicates the initial boundary Γ_I. The objective function is to minimize the generalized compliance under the constraint of allowable material volume, 40% of the original one. The frequency of excitation is $1{,}000\,Hz$ and the following material properties are used: Young's modulus of $195\ GPa$, Poisson's ratio of 0.28, damping factor of 0.1, material density of $7800\,kg/m^3$.

The model A is subject to the rate of internal energy generation of $10^7\,W/m^2$ at the center and the prescribed energy boundary of $0\,J/m^2$ at four corners. Also energy flux of $500W/m$ is applied at the middle of top and bottom sides. The model B is 44 mm long, 44 mm wide, and 1 mm thick. The finite element model is composed of 2,500 plane elements and 2,601 nodes. It is subject to the rate of internal energy generation of $10^7\,W/m^2$ at the center and the prescribed energy boundary of $0\,J/m^2$ at each corner. Also energy flux of $q=200W/m$ is applied at the middle of each side.

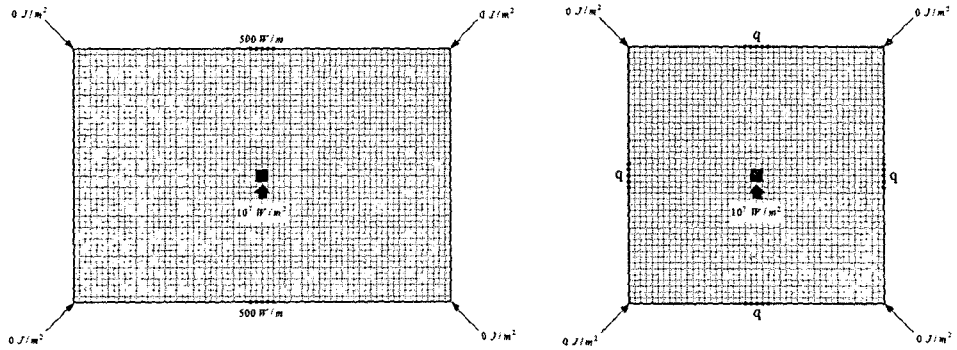

Figure 3 Numerical model A and B

For the model A, Figure 4 shows the histories of implicit boundaries obtained by applying the level set method to the initial design domain without any holes (a), with some holes (b) inside the domain.

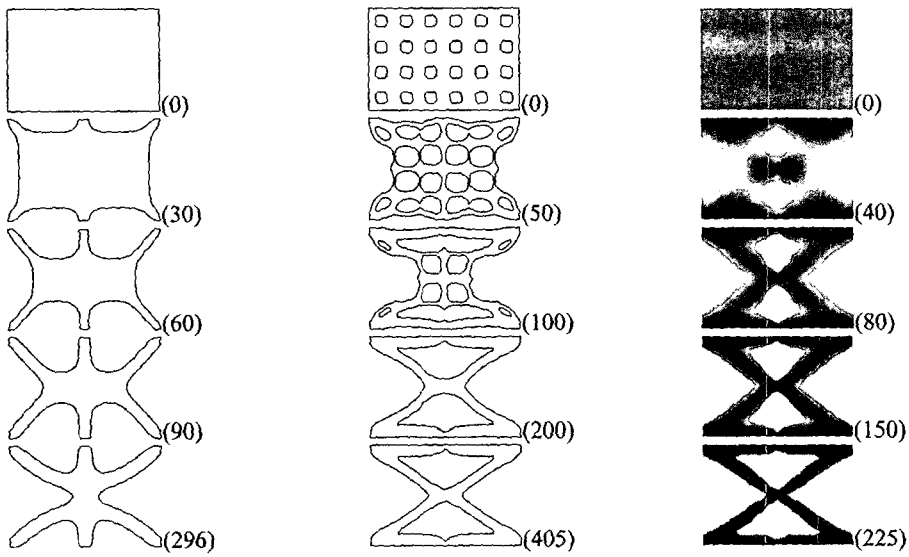

(a) Level set method; (Initial domain without holes)

(b) Level set method; (Initial domain with holes)

(c) Density method

Figure 4 History of shape changes

The (c) shows the result obtained from the established density method. The density method, with the penalty parameter of 2, yields the optimal material distribution at 225 iterations as shown in (c). As shown in (c), a density method suggests a multiply connected topological layout. In level set method, if an initial model has no internal holes, the final optimal shape does not include any internal holes since the developed topology optimization method using the level set method never creates new internal holes. However, the model with initial internal holes can create suitable internal boundary, so the optimal shapes of column (b) and (c) is nearly identical. Thus, we see that the proper initial modeling of the boundary, i.e. the use of sufficient number of holes, is very important for the optimal result. In general, the optimal shape using the level set method is strongly dependent on the initial modeling of the boundary. Figure 5 shows the optimization history without initial holes (a), and with initial holes (b).

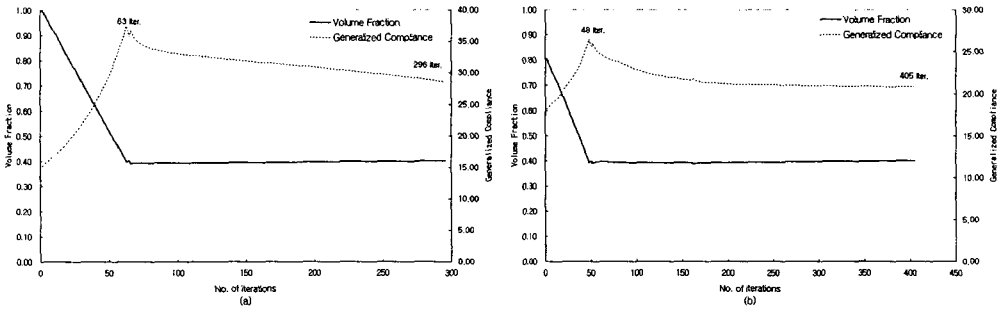

Figure 5 Optimization histories in level set models (a) and (b)

In each case, the volume constraint is satisfied while minimizing the generalized compliance. In Table 1, the generalized compliance and computing cost are compared. The percent agreements of generalized compliance in (a) and (b) with reference to the density method (c) are 133 % and 97 %, respectively. In the case of (a), due to the lack of initial holes, the optimization result is significantly different from the others. Also different generalized compliance is obtained as well. Thus, we notice that the proper initial modeling of the boundary is very important for the optimal result.

Table 1 Comparison of optimization results

	Case (a)	Case (b)	Case (c)
Generalized Compliance	28.55	20.81	21.49
Agreement (%)	132.84	96.83	100.00
Number of Iterations	296	405	225

For the model B in Figure 3, Figure 7 shows the histories of implicit boundaries obtained by applying the level set method to the initial design domain without any holes (A), with some holes (B) inside the domain. The (C) shows the result obtained from the established density method with the penalty parameter of 2. As shown in the row (C), a density method suggests a multiply connected topological layout. In level set method, if an initial model has no internal holes, the final optimal shape does not include any internal holes since the developed topology optimization method using the level set method never creates new internal holes. However, the model with initial internal holes can create suitable internal boundary, so the optimal shapes of row (B) and (C) is nearly identical. Thus, we see that the proper initial modeling of the boundary, i.e. the use of sufficient number of holes, is very important for the optimal result. In general, the optimal shape using the level set method is strongly dependent on the initial modeling of the boundary. Figure 8 shows the connectivity change according to the amount of an applied flux. When no flux is applied, a simple 'X' – shape is obtained as expected. But when some amount of flux is applied, connectivity between flux and temperature boundaries is generated. As the magnitude of flux q is increased, the width of 'X' type braces is decreased but the others increased.

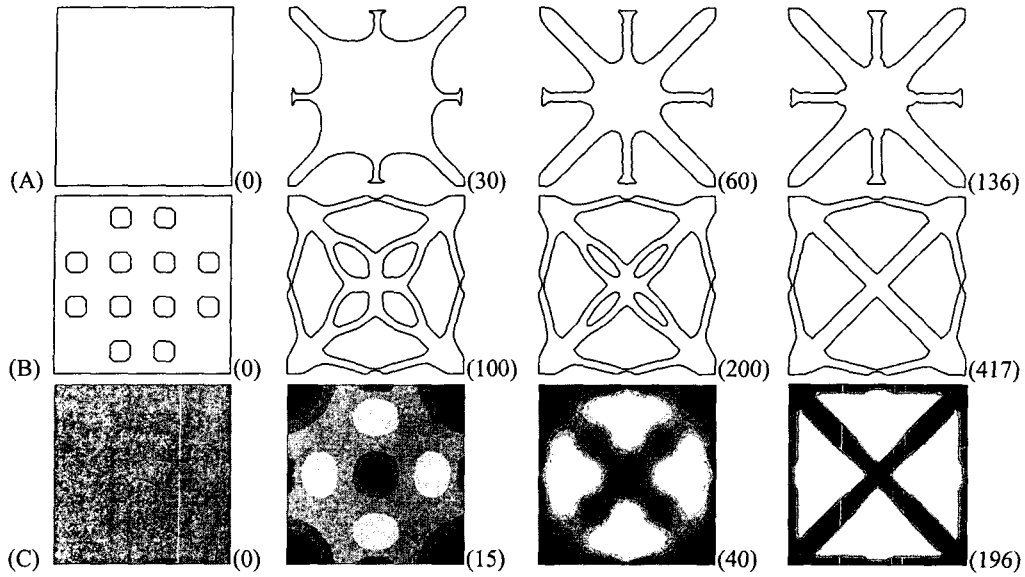

Figure 7 History of shape change

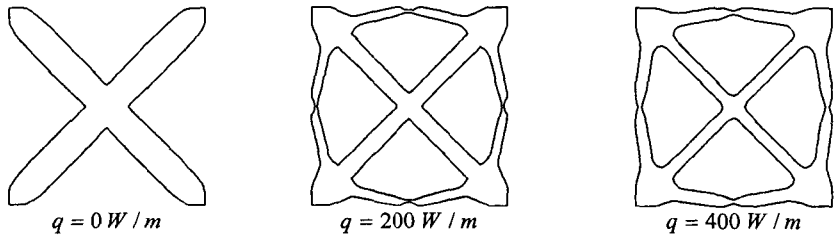

Figure 8 Optimal shapes for various energy flux

5. CONCLUSIONS

A shape optimization method for energy flow problems in steady state is developed using the level set method. Since the implicit moving boundary is used, it is easy to represent the shape variations and there is no need to re-parameterize after significant shape changes during the optimization. Necessary design gradients are computed very efficiently using the adjoint sensitivity analysis method. For the optimization process, the boundary velocity to solve the Hamilton-Jacobi equation is derived from Kuhn-Tucker optimality condition for the Lagrangian function. Some illustrative numerical examples show that the level set method yields the similar optimal shape to the established density approach. Even though the domain experiences significant shape changes, the level set method always gives a smooth boundary. Also, the use of sufficient number of initial holes in the domain is very important to get the reasonable results since this method creates no holes during the optimization.

REFERENCES

1. N.H. Kim, Jun Dong, and K.K. Choi, "Energy flow analysis and design sensitivity analysis of structural problems at high frequencies", *Journal of Sound and Vibration*, Vol. 269, 2004, pp.213-250

2. G. Allaire, F. Jouve, A.M. Toader, "A level-set method for shape optimization", *Numerical Analysis*, Vol. 334, 2002, pp.1125-1130

3. S. Osher, R. Fedkiw, "Level set methods: An Overview and some recent results", *Journal of Computational Physics*, Vol. 169, 2001, pp.475-502

4. M.Y. Wang, X. Wang, D. Guo, "A level set method for structural topology optimization", *Computer Methods in Applied Mechanics and Engineering*, Vol. 192, 2003, pp.227-246